


RESEARCH

Open Access



# Chronic mild stress disrupts mitophagy and mitochondrial status in rat frontal cortex

Cristina Ulecia-Morón<sup>1</sup>, Álvaro G. Bris<sup>1</sup>, Karina S. MacDowell<sup>1</sup>, José L. M. Madrigal<sup>1</sup>, Borja García-Bueno<sup>1</sup>, Juan C. Leza<sup>1</sup> and Javier R. Caso<sup>1\*</sup> 

## Abstract

**Background** Mitochondria are very dynamic organelles that maintain cellular homeostasis, crucial in the central nervous system. Mitochondrial abnormalities have been described in neuropsychiatric diseases, namely major depression disorder (MDD) and schizophrenia. Since stress is the predominant non-genetic cause of MDD, and has a direct impact on mitochondrial networks, understanding how psychological stress affects mitochondrial health is vital to improve the current pharmacological therapies.

**Methods** The effect of 21 days of unpredictable stress was evaluated in frontal cortex of Wistar male rats comparing protein and gene markers of mitophagy (PINK1, PARKIN, BNIP3, NIX, FUNDC1), mitochondrial biosynthesis (PGC1 $\alpha$ , NRF1, TFAM) and dynamics (MFN1, MFN2, OPA1, DRP1), and mitochondrial presence within microglia with the MitoTracker Green FM™ probe.

**Results** Chronic mild stress (CMS) caused the upregulation of mitochondrial mass, mitochondria depolarization, dysregulation in mitochondrial dynamics towards fusion, the increase of mitophagy markers and the induction of genes that activate mitochondrial biogenesis in frontal cortex. CMS also promoted microglia recruitment and mitochondrial number boosting within them.

**Conclusions** There is a dysregulation of mitochondrial dynamics towards fusion, an upregulation of mitophagy markers, and the induction of genes associated with mitochondrial biogenesis in response to CMS in the frontal cortex of adult rats. This study highlights the impact of psychological stress on brain mitochondrial networks.

**Keywords** Mitochondria, Mitophagy, Neuroinflammation, Microglia, Chronic mild stress (CMS)

## Background

Mitochondria are traditionally considered the power station of the cell with a pivotal function in the synthesis of adenosine triphosphate (ATP) [1]. However, that is only the tip of the iceberg: they respond to a wide variety of stress signals (oxidative stress, DNA damage, and pathogens, among others [2–4], control cell fate [5], and regulate cellular homeostasis [6, 7] and immunological processes [8, 9]. Mitochondria adapt their structure, function, and location according to the metabolic state of the cell [10], which is critical in the central nervous system (CNS) [11]. In fact, they modulate neurotransmitter

\*Correspondence:

Javier R. Caso  
jrcaso@med.ucm.es

<sup>1</sup>Departamento de Farmacología y Toxicología, Facultad de Medicina, Universidad Complutense de Madrid (UCM), Centro de Investigación Biomédica en Red de Salud Mental, Instituto de Salud Carlos III (CIBERSAM, ISCIII), Instituto de Investigación Sanitaria Hospital 12 de Octubre (imas12), Instituto Universitario de Investigación Neuroquímica (IUIIN-UCM), Plaza Ramón y Cajal s/n, Madrid 28040, Spain



© The Author(s) 2025. **Open Access** This article is licensed under a Creative Commons Attribution-NonCommercial-NoDerivatives 4.0 International License, which permits any non-commercial use, sharing, distribution and reproduction in any medium or format, as long as you give appropriate credit to the original author(s) and the source, provide a link to the Creative Commons licence, and indicate if you modified the licensed material. You do not have permission under this licence to share adapted material derived from this article or parts of it. The images or other third party material in this article are included in the article's Creative Commons licence, unless indicated otherwise in a credit line to the material. If material is not included in the article's Creative Commons licence and your intended use is not permitted by statutory regulation or exceeds the permitted use, you will need to obtain permission directly from the copyright holder. To view a copy of this licence, visit <http://creativecommons.org/licenses/by-nc-nd/4.0/>.

and calcium ( $\text{Ca}^{2+}$ ) signaling [12], plus intercellular communication at synapses [13].

Mitochondrial impairments lead to an excessive increment of reactive oxygen species (ROS), causing the liberation of mitochondrial DNA (mtDNA) and pro-inflammatory factors [10]. Growing evidence links oxidative stress and neuroinflammation to neuropsychiatric diseases [14–16]. A meta-analysis study found that patients with major depressive disorder (MDD) had elevated levels of cortisol, the stress hormone, in response to psychosocial stress in comparison to healthy controls [17, 18]. Mitochondria possess glucocorticoid receptors (GR) and are sensitive to systemic cortisol levels [19], which in turn adapt oxidative phosphorylation gene expression and energy metabolism [20]. Additionally, patients with mitochondrial diseases or mutations in the mtDNA present comorbidities of psychiatric symptoms [21–23].

When metabolic or environmental stresses reach a certain point, mitochondrial fusion and fission allow the cell to preserve healthy mitochondria: whereas fission mediates the division of one mitochondrion into two, making it possible to eliminate damaged parts through apoptosis [24] or mitophagy [25], fusion promotes the merge of two mitochondria with the purpose of mitigating partially impaired mitochondria [24]. Membrane GTPases mitofusin 1 (MFN1) and mitofusin 2 (MFN2), together with optic atrophy protein 1 (OPA1) oversee the fusion process. The GTPase dynamin-related protein 1 (DRP1) is recruited to induce mitochondrial fission [26]. A lower expression levels of MFN2 has been linked to the modulation of anxiety and depression-like behaviors in Wistar rats [27].

When mitochondria malfunction to such an extent that need to be removed, they are cleared away via the ubiquitin-dependent or independent mitophagy pathway [10]. The phosphatase and tensin homologue-induced putative kinase 1 (PINK1) and PARKIN orchestrate the ubiquitin-dependent mitophagy pathway: in response to several stimuli, PINK1 is cleaved onto the outer mitochondrial membrane (OMM) [28], which consequently causes its autophosphorylation and PARKIN translocation to the OMM from the cytosol [29]. Then, PARKIN mediates the ubiquitination of several substrates on the defective mitochondria. This constitutes a signal to recruit mitophagy adaptors (i.e., the sequestosome SQSTM1/p62 or optineurin) which will mediate the enclosure of mitochondria within the mitophagosome and their transport to the lysosome [30]. FUN14 domain containing 1 (FUNDC1), BCL2 interacting protein 3 (BNIP3), and BCL2 interacting protein 3 like (BNIP3L/NIX) are OMM mitophagy receptors that directly induce ubiquitin-independent mitophagy [29], which is activated in response to stress [31]. Both pathways interact, since BNIP3 and NIX also control PARKIN recruitment and translocation [32, 33].

Studies have highlighted the role of mitochondrial dysfunction in the pathophysiology of MDD [31, 34, 35] and antidepressant actions [36]. Some have demonstrated the activation of mitophagy for the alleviation of depressive-like symptoms produced by models of depression-like behavior in rodents [37, 38]. To better understand how chronic stress can influence mitochondrial status in the CNS, we carried out an environmental model of depression-like behavior in rats, and evaluated mitophagy, mitochondrial dynamics, and biogenesis markers in the frontal cortex (FC), since it is one of the most vulnerable brain regions affected by MDD [39]. Besides, as microglia are key in the stress response, microglia were isolated, and their mitochondria quantified after CMS exposure. We aimed to explore whether stress modulates these processes and how they could be modulated to improve therapeutic strategies for stress-related diseases.

## Methods

### Experimental design

Male Wistar Hannover rats (HsdRccHan: Wist, ENVIGO, Spain) weighing 200–225 g were individually caged and kept under temperature and humidity standard conditions, with a 12 h light/dark cycle (8:00 h–20:00 h) and food and water *ad libitum* for 14 days prior to the stress. Procedures followed the Animal Welfare Committee of the Complutense University and Madrid Regional Government guidelines (PROEX098/19) according to European legislation (2010/63/EU). Studies are reported in compliance with the ARRIVE guidelines and all efforts were focused on minimizing the suffering and reducing the number of animals employed.

Rats were randomly divided into two experimental groups: control (CT) and chronic mild stress (CMS), whose sample size varies according to the specific determination and is specified in next sections.

### CMS protocol

The CMS protocol is a modification from the one described by Willner [40]. Our group has previously demonstrated how this protocol induces a depressive-like behavior evaluated by several behavioral tests (i.e., sucrose, forced-swim, splash, and elevated plus maze tests) [41]. For 21 days, seven-week-old rats were exposed to two alternating stressors every 12 h. These included soiled bedding, food/water deprivation, cage tilting, paired housing, stroboscopic and/or intermittent illumination. Sample collection was conducted two days after protocol finalization.

### Sample collection

Samples were collected between 13:00 h–15:00 h to mitigate circadian rhythms influence through terminal anesthesia with sodium pentobarbital (320 mg/kg i.p.,

Vetoquinol®, Spain) or cervical dislocation. The latter was only used for the flow cytometry approach, to avoid potential biochemical interference. Brains were extracted from skulls and the FC was isolated. For immunoblotting and mRNA analyses, tissue was directly frozen at -80 °C; for immunostaining, brains were perfused and fixed with 4% paraformaldehyde; for enzymatic assays and flow cytometry, brain tissue was placed in cooled PBS 1 × (137 mM NaCl, 2.7 mM KCl, 10 mM Na<sub>2</sub>HPO<sub>4</sub>, and 1.8 mM KH<sub>2</sub>PO<sub>4</sub> in 1 L of dH<sub>2</sub>O, pH = 7.4) with phosphatase and protease inhibitors (Roche, 4906837001 and 11697498001), or DMEM/F-12 GlutaMAX media (Fisher Scientific, 31331028) with antibiotics (Life Technologies, 15070063) respectively (see Supplementary data for details).

**Determination of malondialdehyde (MDA), 8-hydroxy-2-deoxyguanosine (8-OHdG), and catalase**

Total homogenates from FC samples were deproteinized with trichloroacetic acid and hydrochloric acid (HCl), and then mixed with 2% thiobarbituric acid (TBA) in 0.5 N of NaOH. Homogenates were incubated in a water bath for 15 min at 90°C. Afterwards, they were centrifuged at 12,000 × g for 15 min at 4°C. Supernatants were collected, and their MDA levels were measured at 532 nm using the Synergy microplate reader (BioTek, USA). Internal controls were added to ensure MDA measurements.

Oxidative stress damage to nucleotides was evaluated by quantifying the 8-OHdG levels using a DNA Damage kit (Arbor Assays, K059-H1). Functional activity of catalase was examined with the Catalase Colorimetric

Activity kit (Arbor Assays, K033-H1) (see Supplementary data for details).

**Tissue homogenization and Western blot (WB)**

Cytosolic fractions were isolated without nuclear contamination [42]. Mitochondrial fractions were obtained by using a kit for mitochondrial isolation (Sigma-Aldrich, MITOISO1).

The Bradford assay was conducted, and once protein levels were quantified, they were loaded into SDS-polyacrylamide gels to perform electrophoresis (100 V). Antibodies (Table 1) were revealed with ECL® kit (Fisher Scientific, 12994780) using the Odyssey® Fc System (LICOR Biosciences). The loading housekeeping control was β-ACTIN (Sigma-Aldrich, A5441). They were quantified by densitometry employing the NIH ImageJ® software. The number of animals used was CT (n = 7) and CMS (n = 14) (see Supplementary data for details).

**RNA extraction and RT-qPCR analyses**

Total RNA was extracted from FC with TRIzol® reagent (Invitrogen, 15596018) and homogenized using the TissueLyser LT (Quiagen, Netherlands). Aliquots of each sample were processed to cDNA using random hexamer primers (Invitrogen, 48190011). Quantitative changes in mRNA levels were detected by real-time (RT) quantitative polymerase chain reaction (qPCR) in the presence of SYBR Green (Biotools, 10606–4153) fixing the following conditions in a Corbett Rotor-Gene (Corbett Research, Australia): 35–40 cycles of denaturation at 95 °C (10s), annealing at 63 °C (15s), and extension at 72 °C (20s). *Tubulin-α* gene expression was employed as housekeeping gene to normalize the results. To ensure the stress protocol did not influence *Tubulin-α* and *Gapdh* gene expression, BestKeeper software was used. Melt curves were all evaluated to specifically recognize single gene transcripts. Gene expression was assessed by a Comparative Quantification method [43]. Triplicate measurements of each aliquot were loaded, together with a negative internal control in each run. Primers are listed in Table 2. The same number of animals as in the previous section was employed.

**Immunofluorescence (IF)**

Brain slices were incubated with glycine 100 mM (AppliChem, A1067) in potassium phosphate buffer (KPBS) and then blocked in 10% BSA and 0.3% Triton X-100 (Sigma-Aldrich, T8787). Then, primary antibodies were incubated 48–72 h in agitation at 4°C (Table 3). After secondary antibody incubation, 4',6-diamidino-2-phenylindole dihydrochloride (DAPI; Sigma-Aldrich, MBD0015) was added for 4 min. Slices were laid on slides with Fluoroshield® (Sigma-Aldrich, F6182) and cover slipped. Confocal images were obtained employing a Confocal Leica

**Table 1** Antibodies and dilutions for Western blot determinations. Abcam (ab), Cell Signaling technology (CS), Santa Cruz technologies (sc), and Sigma-Aldrich (SA)

Protein (molecular weight)	Primary antibody (dilution)
PARKIN (55 kDa)	ab77924 (1:1000)
PINK1 (66 kDa)	ab23707 (1:1000)
BNIP3 (22–28 kDa)	CS, 3769 (1:1000)
NIX (38 kDa)	CS, 12396 (1:1000)
FUNDC1 (17 kDa)	SA, ABC506 (1:1000)
AMBRA1 (135 kDa)	CS, 24907 (1:500)
UBIQUITIN	CS, 3936 (1:1000)
NRF1 (30 kDa)	sc-28379 (1:750)
MTFA (25 kDa)	sc-166965 (1:750)
PGC1α (92–105 kDa)	ab54481 (1:1000)
MITOFUSIN 1 (MFN1) (84 kDa)	ab126575 (1:750)
MITOFUSIN 2 (MFN2) (80 kDa)	CS, 9482 (1:1000)
OPA1 (80–100 kDa)	CS, 80471 (1:1000)
phospho-DRP1 (78 kDa)	CS, 6319 (1:750)
DRP1 (78 kDa)	CS, 5391 (1:1000)
TOMM20 (16 kDa)	CS, 42406 (1:1000)
β-ACTIN (42 kDa)	SA, A5441 (1:10000)

**Table 2** Sequences of primers to target genes of interest

Gene	Forward primer (5'-3')	Reverse primer (3'-5')
<i>Parkin</i> (NM_020093)	CTGGCAGTCATTCTG-GACAC	CTCTCCACT-CATCCGTTTG
<i>Pink1</i> (NM_001106694)	CATGGCTTTGGATG-GAGAGT	TGGGAGTTT-GCTCTTCAAGG
<i>Snip3</i> (NM_053420)	GATTGGATATGGGATTGG	CAGATGAGA-CAGTAACAG
<i>Nix</i> (NM_080888)	TGGAGCCAT-GAAGAAAGGGG	CAGAAGGTGT-GCTCAGTCGT
<i>Fundc1</i> (NM_001025027)	TATTTGGCCACAGTTC-CGGA	AGAAAACCAC-CACCTACTGCA
<i>Nrf1</i> (NM_001100708)	TGCTTCAGAACTGC-CAACCA	GGTCATTTAC-CGCCCTGTA
<i>Mtfa</i> (NM_031326)	ACACCAGATG-CAAAAGTTTCA	TGTACACCTTC-CACTCAGCT
<i>Pgc1a</i> (NM_031347.1)	CAGTCCTTCTCCAT-GCCTG	CTGTGGGTGTG-GTTTGATG
<i>Mfn2</i> (NM_130894.4)	TGCCTGGATGCTGAT-GTGTT	TCCATGTACT-CAGGCTCCGA
<i>Mfn1</i> (NM_138976.1)	TGGCATCCCTCACGTC-TAGA	GCTCTCTCTTTC-GCAGAGT
<i>Opa1</i> (NM_133585.3)	AAGGAGGCTGT-GAAGGAGGA	TGCGTCCCACT-GTTGCTTAT
<i>Drp1</i> (NM_053655.3)	TCTCAAGGTTTCTC-GCCCA	GTGCCTCTGAC-GTTGCCATA
<i>Ambra1</i> (NM_001134341.3)	GAGCAGGATCCAGAGA-GCAC	TCTGTTG-GTAGCGCATG-GAG
<i>Rnr1</i> (NC_001665.2)	TGAAGCG-GAAAGAAATGGGC	AATTTGAG-GAGGGTGAC-GGG
<i>Nd1</i> (NC_001665.2)	GCAGGACCATTC-GCCCTATT	GGGGTAGGAT-GCTCGGATTC
<i>Nd5</i> (NC_001665.2)	ATTCCGCAGTCTGGGT-TAGC	TGGAGAGAG-GAGGAAAGGGG
<i>Tubulin-α</i> (NM_022298)	CCCTCGCCATGGTA-AATACAT	ACTGGATGG-TACGCTTGGTCT
<i>Gapdh</i> (NM_017008.4)	ATGGTGAAGGTCGGT-GTGAA	TGACTGTGCC-GTTGAACCTG

**Table 3** Primary and secondary antibodies with respective dilutions for Immunofluorescence approaches

Protein	Primary antibody (dilution)	Secondary antibody (dilution)
PARKIN	ab77924 (1:100)	Alexa Fluor 555, A31570 (1:850)
NeuN	ab177487 (1:800) / ab104224 (1:800)	Alexa Fluor 488, A21206 (1:850) / Alexa Fluor 555, A31570 (1:850)
TOMM20	ab186735 (1:100)	Conjugated Alexa Fluor 555
IBA1	ab5076 (1:850)	Alexa Fluor 555, A21432 (1:850)

SP8 Microscope, in the CAI-UCM *Centro de Citometría y Microscopía de Fluorescencia* (see Supplementary data for details).

### Immunoprecipitation (IP)

The Pierce® Co-Immunoprecipitation kit (ThermoFisher, 26149) was employed. Once the eluted PARKIN-enriched samples were obtained, 20 µl were loaded and revealed against anti-UBIQUITIN antibody (Cell Signaling, 3936, 1:1000). The loading control was β-ACTIN. The IP experiments were repeated three times with different animals, each round with CT ( $n=3$ ) and CMS ( $n=3$ ) (see Supplementary data for details).

### Flow cytometry

Freshly collected FC of rat brains were pooled (the FC from two animals of the same group made one pool) in DMEM/F-12 GlutaMAX (Fisher Scientific, 31331028) supplemented with antibiotics (Life Technologies, 15070063). Microglial isolation was performed by enzymatic digestion in PBS supplemented with 2% fetal bovine serum (FBS) (Gibco, 10438026) and 0.02% glucose (Sigma-Aldrich, G8644), during 30 min at 37°C. After stopping the enzymatic digestion with 10% FBS in DMEM/F-12, mechanical digestion was applied by gently pipetting cellular suspension, which was then filtered with 40 µm cell strainers (Falcon™, 352350). Afterwards, samples were centrifuged at 600  $\times$  g for 10 min at 4°C. Supernatants were removed and 37% Percoll™ (Cytiva, 17089101) in PBS was cautiously added. A density gradient was formed after 20 min centrifugation at 350g and 4°C. The intermediate, white phase was removed, and more PBS was added to wash the cells. After another centrifugation, samples were incubated with MitoTracker Green FM™ (Invitrogen, M4675) for 20 min at 37°C in the dark. Afterwards, they were incubated with FcyII (BD Bioscience, 550270) for 10 min at 4°C in the dark. CD45 (BD Biosciences, 559135) and CD11b (BD Biosciences, 562105) antibodies (1:50 dilution) were subsequently added and incubated for 10–15 min at 4°C in the dark. Hoechst (Invitrogen, H3569) (1:1000 dilution) was added after antibodies removal. All samples were measured by BD FACSARIA III™ flow cytometer in the previously mentioned CAI-UCM. See Supplementary data for more information.



### Statistical analyses

Data are expressed as mean  $\pm$  SEM in both text and figures. Outliers were identified using the ROUT method. To examine Gaussian distribution, the Shapiro Wilk normality test was applied. When the sample distribution was normal, a two-tailed unpaired Student's *t*-test was applied, comparing CT vs. CMS. If the sample distribution was not normal, a two-tailed non-parametric Student's *t*-test was employed using the Mann-Whitney test. A *p* value  $< 0.05$  was considered statistically significant.

## Results

### CMS induced lipid peroxidation and unbalanced the antioxidant defense, and promoted mitochondrial depolarization

To assess the oxidative profile after CMS exposure, lipid peroxidation was first evaluated via MDA concentration, which is a key biomarker of damage caused by oxidative/nitrosative stress. MDA levels were higher in CMS when compared to CT (Fig. 1A). To further elucidate if CMS generated an aberrant oxidation of nucleic acids, 8-OHdG levels (a biomarker of DNA damage caused by reactive oxygen species) were measured, although no differences were observed (Fig. 1B). Regarding the antioxidant defense, the enzyme catalase was found reduced in the CMS group (Fig. 1C). To evaluate if CMS affected mitochondrial genes, the transcription of the mitochondrial genes *Rnr1*, *Nd1*, and *Nd5* was compared to the genomic gene *Gapdh*, but no changes were observed between the two groups (Fig. 1D). At the protein level, the translocase of the outer mitochondrial membrane complex subunit 20 (TOMM20) was evaluated to study the impact of CMS on mitochondria quantity, which showed a considerable increase, evaluated both by WB and IF (Fig. 1E and G). TOMM20 was present in a higher concentration in neuronal somas (Fig. 1G). Lastly, JC-1 was assayed to evaluate mitochondrial function and transmembrane membrane potential ( $\Delta\psi_M$ ), which displayed a clear decrease of the dye concentration after CMS exposure (Fig. 1F).

### Mitochondrial dynamics was altered by CMS

Mitochondrial dynamics, fusion, and fission processes were examined through its main proteins in both cytosolic (gray) and mitochondrial (red) fractions (Fig. 2). MFN1 and MFN2 protein levels were downregulated in the CMS when compared to the CT group in the cytosolic fraction. DRP1 protein presence decreased after CMS exposure (Fig. 2A). Fusion proteins MFN2 and optic atrophy-1 (OPA1) were upregulated in the

mitochondrial-enriched fraction, as well as the phosphorylation of DRP1 (Fig. 2B). The same markers were studied by RT-qPCR (Supplemental Fig. S1C), but only *Mfn1* showed modifications at the transcriptional level, whose gene expression was enhanced after the CMS (Fig. 2C).

### CMS boosted mitophagy proteins in the mitochondrial fraction

To analyze mitochondrial turnover, both PINK1-PARKIN-dependent and receptor-mediated mitophagy were evaluated. PARKIN displayed an upregulation in the cytosolic fraction of the CMS group. Regarding receptor-mediated mitophagy, BNIP3 was upregulated when compared to the CT group, whereas FUNDC1 protein levels decreased (Fig. 3A). In the mitochondrial fraction, PINK1 protein was found highly augmented. Receptor-mediated mitophagy was promoted after CMS, since BNIP3, BNIP3L/NIX, and FUNDC1 protein concentrations were increased (Fig. 3B). No changes were observed in AMBRA1 protein levels. Immunofluorescence studies revealed that CMS-mediated alterations of PARKIN were mainly taking place in neurons (Fig. 3C). Additionally, PARKIN was immunoprecipitated and incubated with an anti-UBIQUITIN antibody to assess its polyubiquitination: CMS-exposed rats exhibited a more intensified polyubiquitination profile than controls. Moreover, CMS showed higher concentrations of PARKIN in the eluted fraction after the immunoprecipitation (Fig. 3D).

### CMS promoted the transcription of mitochondrial biogenesis genes

Mitochondria biogenesis was studied through its main orchestrators at the mRNA and protein levels. In nuclear fractions, nuclear respiratory factor 1 (NRF1), mitochondrial transcription factor A (MTFA), and peroxisome proliferator-activated receptor  $\gamma$  coactivator  $\alpha$  (PGC1 $\alpha$ ) showed a subtle tendency towards a lower protein presence after CMS. PGC1 $\alpha$  protein concentration increased in the cytosolic fraction compared to the nuclear one after CMS exposure (Fig. 4A). At the mRNA level, *Nrf1* and *Pgc1 $\alpha$*  transcription was promoted by the CMS, and *Mtfa* exhibited a similar tendency pattern (Fig. 4B).

### Microgliosis: mitochondrial mass was higher within microglia after CMS

Given the role of microglia in the fight against oxidative stress, mitochondrial status in freshly isolated populations of microglia were examined. Immunofluorescence analysis showed an increase of the microglia marker IBA1

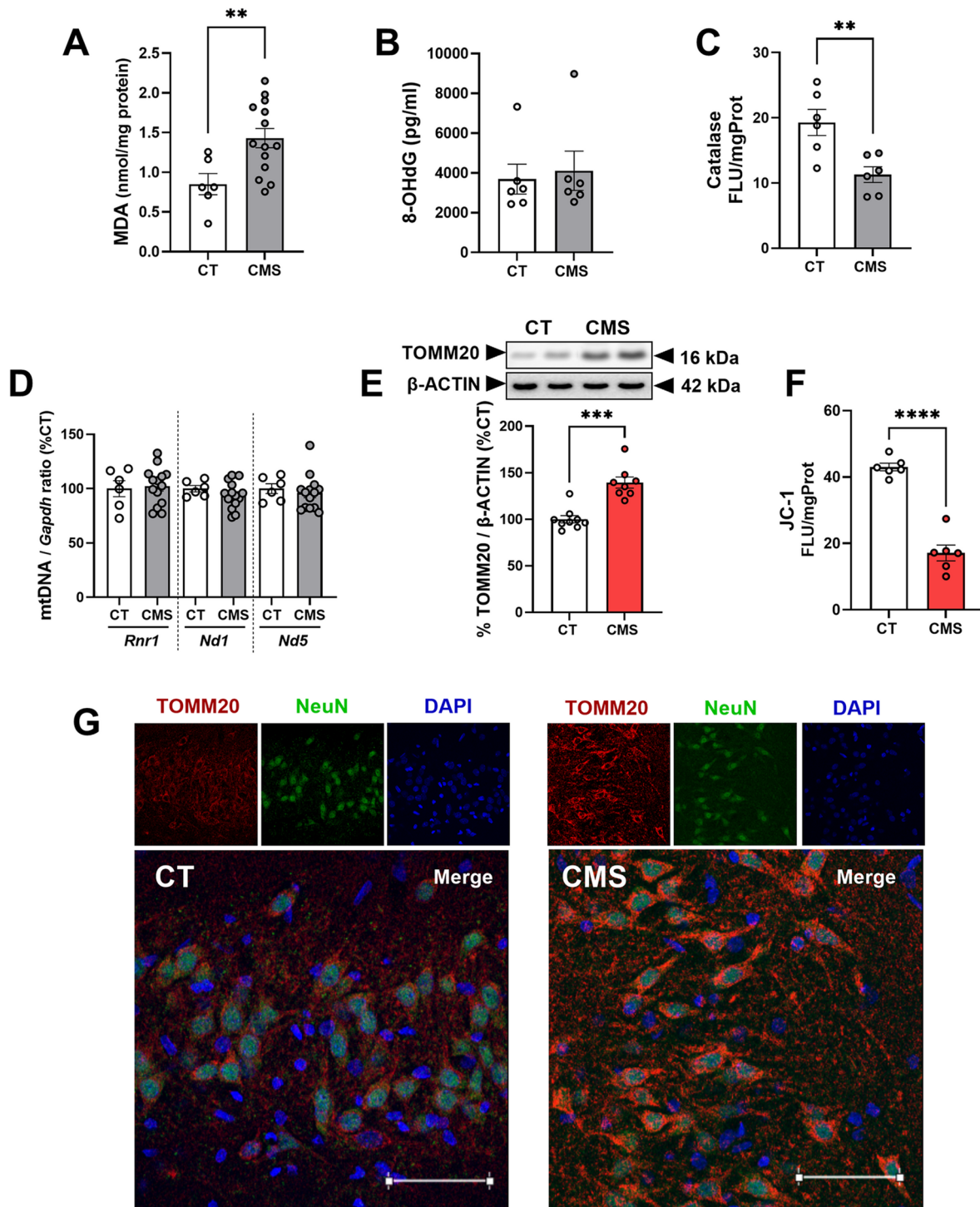


**Fig. 1** Evaluation of CMS-derived oxidative stress and mitochondrial status in frontal cortex. Cortical levels of lipid peroxidation in CT and CMS groups were measured and compared via the analysis of malondialdehyde concentration (**A**). Nucleotide damage caused by ROS was examined (**B**), as well as the antioxidant enzyme catalase (**C**). Transcriptional levels of mitochondrial genes *Rnr1*, *Nd1*, and *Nd5* were studied and compared to *Gapdh* (**D**). Mitochondrial mass was assessed through the analysis of TOMM20 protein expression in mitochondria-enriched fractions (**E**). JC-1 assay was also performed to evaluate alterations in the mitochondrial transmembrane potential (**F**). TOMM20 immunostaining confirmed its increment in the CMS group, which was accumulated mainly in neuronal somas. Scale bars represent 50 μm (**G**). Two-tailed Student *t*-test was used for statistical analyses. Data is expressed as mean ± SEM of 6–14 CT and CMS rats. (\*\**p* < 0.01, \*\*\**p* < 0.001, \*\*\*\**p* < 0.0001)

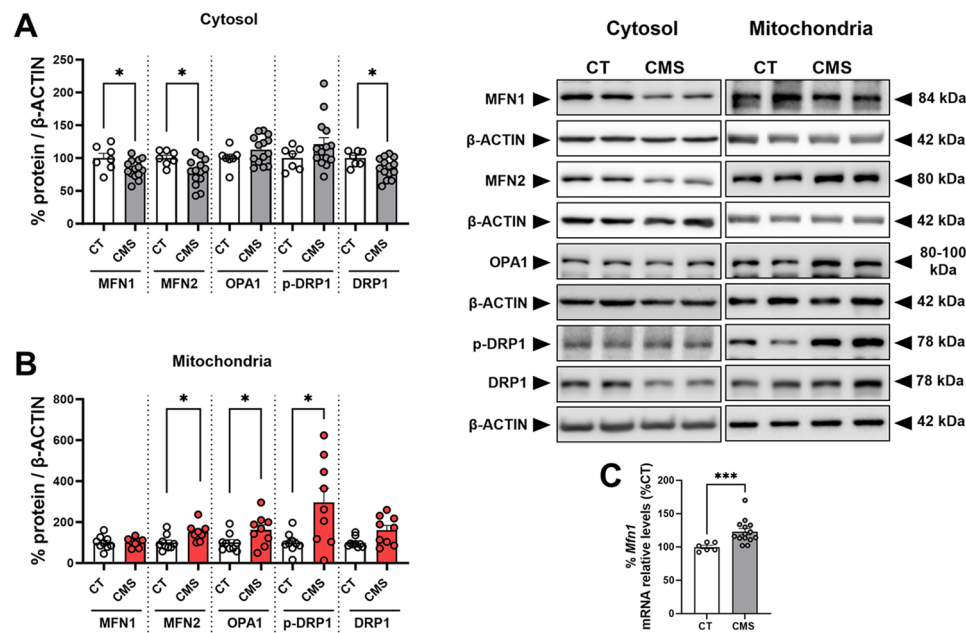


**Fig. 2** Mitochondrial dynamics characterization in cytosolic and mitochondrial subcellular fractions from frontal cortex of rats. Protein changes in cytosolic extracts are shown in (A), whereas alterations in mitochondrial-purified fractions are displayed in (B). Although all these markers were also studied by RT-qPCR, only *Mfn1* showed CMS-related modifications (C). Two-tailed Student *t*-test was used for statistical analyses. Data is expressed as mean  $\pm$  SEM of 6–14 CT and CMS rats. (\*\*\*) $p < 0.001$

in the CMS group (Fig. 5A). Furthermore, microglia were purified from FC, and their mitochondria specifically stained and examined by flow cytometry (Fig. 5B–D). CD45<sup>medium</sup> and CD11b<sup>high</sup> double stain allowed the isolation of the microglial population, which was indeed increased in the CMS group (Fig. 5E). Among this population, MitoTracker Green FM™ displayed a higher presence in CMS-upregulated microglia (red), compared to control microglia (blue) (Fig. 5F). Gating strategy is summarized in Supplemental Fig. S2.

## Discussion

In this work, many aspects of mitochondrial homeostasis have been assessed in the FC of rats subjected to a model of depressive-like behavior. Three-week exposure to a well-known preclinical protocol of depressive-like behavior caused an increase of the mitochondrial mass, the alteration of mitochondrial transmembrane potential ( $\Delta\psi_M$ ), and mitochondrial dynamics, in addition to the increase of mitophagy proteins and mitogenesis-related gene-transcripts in this brain region. Moreover, CMS led to microglial accumulation and the boost of their mitochondrial mass.

Regarding oxidative stress, CMS caused lipid peroxidation in cellular membranes [42, 44], lower levels of the enzyme catalase, and no oxidative nucleic acid damage, although the chronicity of the stress might eventually contribute to oxidative DNA damage [45].

The stress response needs energy to ensure that all the adaptive/coping mechanisms fighting against the stressor will succeed [46], so that the increment of mitochondrial mass, measured by the concentration of the translocase TOMM20, would give the cell the response for this extra energy demand. However, the JC-1 dye, whose intensity ratio is solely dependent on mitochondrial membrane potential, exhibited a CMS-derived alteration of  $\Delta\psi_M$ , being the reduction of its concentration inside mitochondria a direct indicator of depolarization and poor cellular health [47]. The increase of TOMM20 might be a compensatory mechanism for a reduced mitochondrial  $\Delta\psi_M$ , so additional translocases, as well as their activity, should be explored in the future to fathom this result.

Despite depolarized mitochondria being unable to fuse one another [48], fusion proteins MFN2 and OPA1 increased in mitochondrial extracts, while the inhibitory phosphorylation of DRP1 was induced by CMS. This indicates that CMS promoted the fusion process, possibly as a cellular attempt to reduce damaged components of depolarized mitochondria by merging them with healthier ones, or as a strategic survival option, by mixing mitochondrial components and hence restore mitochondrial integrity [49]. The lower cytosolic presence of mitofusins, either because of an increased mitochondrial translocation or a higher proteasome degradation [50, 51], would support this notion.



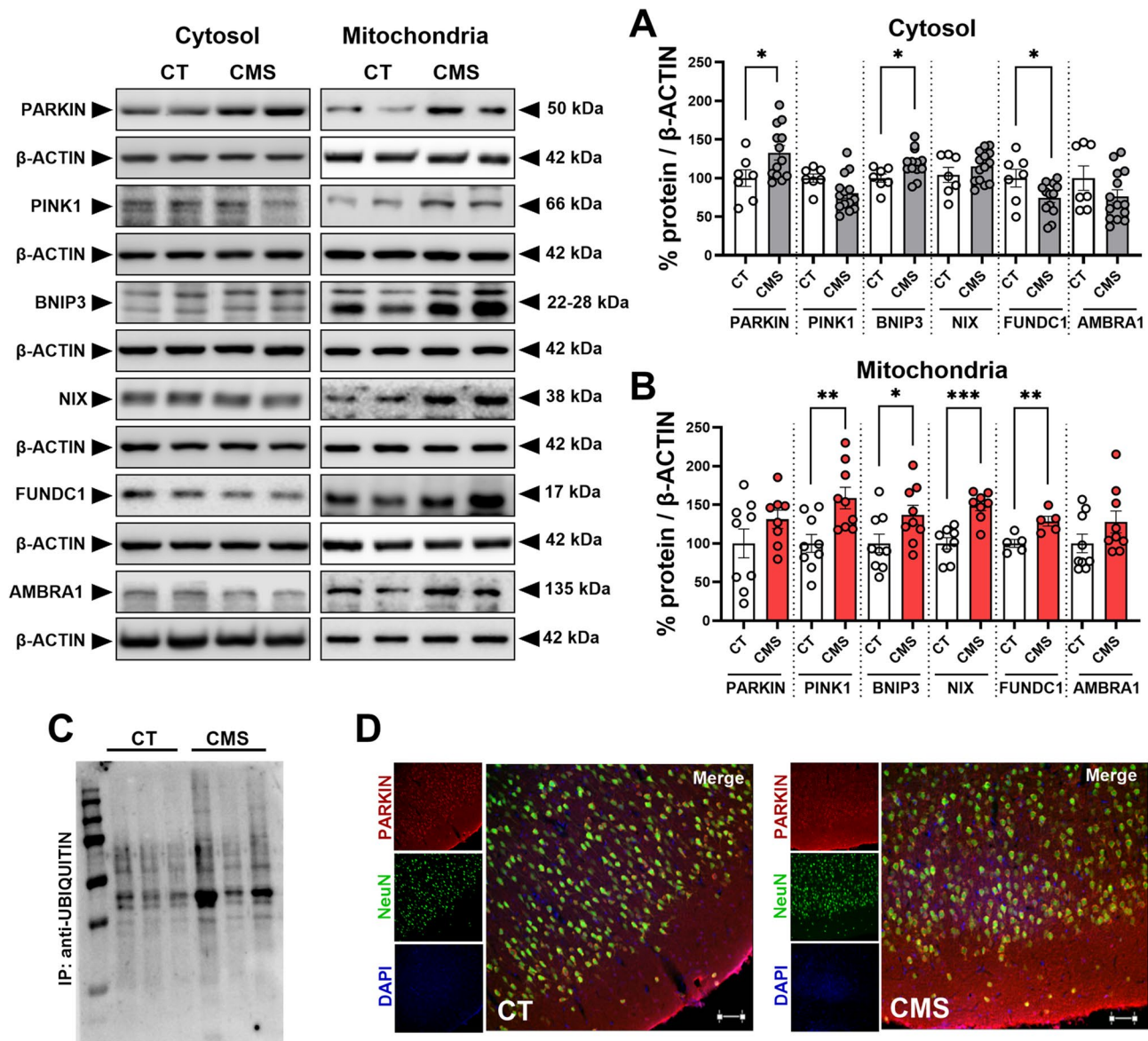


**Fig. 3** Study of mitophagy markers in cytosolic and mitochondrial subcellular fractions and PARKIN-mediated polyubiquitination after CMS exposure. PINK1-PARKIN dependent and receptor-mediated mitophagy were explored in cytosolic extracts (A) and in mitochondrial-enriched fractions of rat frontal cortices (B). PARKIN immunostaining was carried out with the neuronal marker NeuN. Scale bars represent 50  $\mu$ m (C). PARKIN was immunoprecipitated and then incubated and revealed against an anti-UBIQUITIN antibody. Each lane represents one animal ( $n = 3$  per group) (D). Two-tailed Student *t*-test was used for statistical analyses. Data is expressed as mean  $\pm$  SEM of 6–14 CT and CMS rats. (\*\* $p < 0.01$ , \*\*\* $p < 0.001$ )

In case of a fission impairment and the upregulation of fusion proteins, depolarized mitochondria could be forced into fusion events [52]: OPA1 upregulation might be the cellular response to reinstate inner membrane integrity, even in depolarized mitochondria [53]. *Mfn1* transcriptional upregulation may be indicative of a specific cellular response to promote outer membrane fusion. While MFN1 has higher GTPase activity and might be preferentially induced when rapid fusion is required [54], MFN2 is more involved in mitochondria-ER networks and signaling [55, 56].

To ensure the preservation of healthy mitochondria, asymmetric fission gives rise to two new mitochondria, one depolarized and another completely polarized. Then, mitophagy clears out depolarized mitochondria to preserve cellular homeostasis [57]. CMS boosted receptor- and PINK1-PARKIN-mediated mitophagy proteins in the mitochondrial fraction, which points to the induction of the pathway, both dependent and independent of ubiquitin. Higher cytosolic PARKIN concentrations could be a counterresponse to an enhanced mitochondrial dysfunction, since PARKIN has many roles beyond

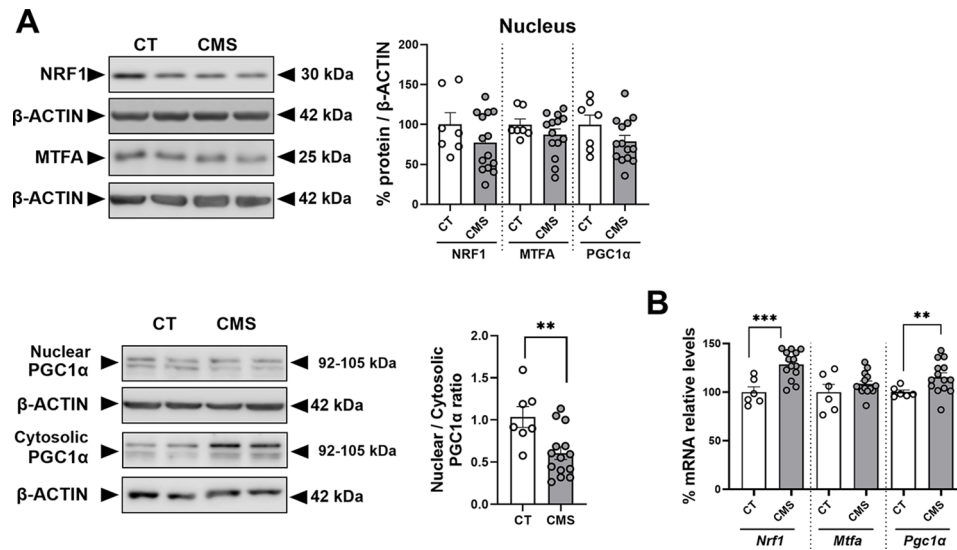


**Fig. 4** Analysis of CMS-derived alterations in mitochondrial biogenesis markers in frontal cortex of rats. Nuclear fractions were used to study protein presence of NRF1, MTFA, and PGC1 $\alpha$ . Cytosolic protein concentrations of PGC1 $\alpha$  were higher than in the nuclear fraction (**A**). *Nrf1* and *Pgc1a* gene inductions were observed, the same tendency in *Mtfa* (**B**). Two-tailed Student t-test was used for statistical analyses. Data is expressed as mean  $\pm$  SEM of 6–14 CT and CMS rats. (\*\* $p$  < 0.01, \*\*\* $p$  < 0.001)

mitophagy, especially under stress conditions [58]. On top of that, PARKIN protein elevations in both compartments might highlight the inefficient disposal of damaged mitochondria, reflecting an obstruction in the autophagy machinery.

Polyubiquitinated mitochondria are a target for mitophagy receptors, and PARKIN mediates the ubiquitination of many of the outer mitochondrial membrane proteins [59]. The immunoprecipitation of PARKIN and subsequent incubation with an anti-UBIQUITIN antibody revealed that CMS contributed to a higher polyubiquitination profile. This points to CMS-derived damaged mitochondria and PINK1-PARKIN activation, suggesting that the ubiquitin-proteasome pathway and mitophagy are actively engaged in response to mitochondrial stress or dysfunction after CMS exposure.

BNIP3, NIX, and FUNDC1 protein concentrations were enhanced in mitochondrial extracts after CMS exposure. Their increment implies that mitochondria are being targeted for degradation more frequently. BNIP3 and FUNDC1 are recruited under low oxygen, nutrient deprivation, or excessive ROS conditions [60–62], which may indicate that chronic stress reduces oxygen supply or disrupts mitochondrial function in the brain. Considering that ATP production is impeded in dysfunctional mitochondria, CMS could have altered ATP biosynthesis [63, 64], and thus, the induction of BNIP3/NIX and FUNDC1-mediated mitophagy would help remove them.

Future experiments should tackle the apparent contradictory results of CMS-derived simultaneous increased

fusion and mitophagy. This phenomenon might be a coordinated quality control mechanism, in which fusion promotes content exchange and repair while mitophagy favors mitochondrial damaged components removal. Furthermore, an experimental design based on the use of prolonged periods of stress would allow to explore the modulation of the pathway and help determine whether adaptive phenomena occur.

A deficient mitophagy process might not be the only reason for impaired mitochondrial accumulation: a higher rate of mitochondrial biogenesis could have overcompensated for the dysfunctional mitochondria. This hypothesis does not exclude what is aforementioned: mitophagy and mitogenesis keep intracellular balance, so the overproduction of new mitochondria could have also stimulated mitophagy initiators [64]. PGC1 $\alpha$  is the main orchestrator in the synthesis of mitochondria *de novo* through the induction of NRF1 and TFAM, which favors mtDNA replication and transcription [65]. Nuclear protein presence of these three markers was unaltered, in the case of PGC1 $\alpha$  owing to a lower translocation ratio to the nucleus. Hence, elevated cytosolic PGC1 $\alpha$  concentration could imply a hindrance in the transcriptional activation of downstream genes.

CMS caused the induction of *Pgc1a* and *Nrf1*, whose translation would eventually result in higher levels of their proteins to finally contribute to mitochondrial biosynthesis [64]. Overall, CMS-mediated protein reduction of PGC1 $\alpha$  in the nuclei extracts might have slowed down the activation of downstream *Nrf1* and *Mtfa*, being



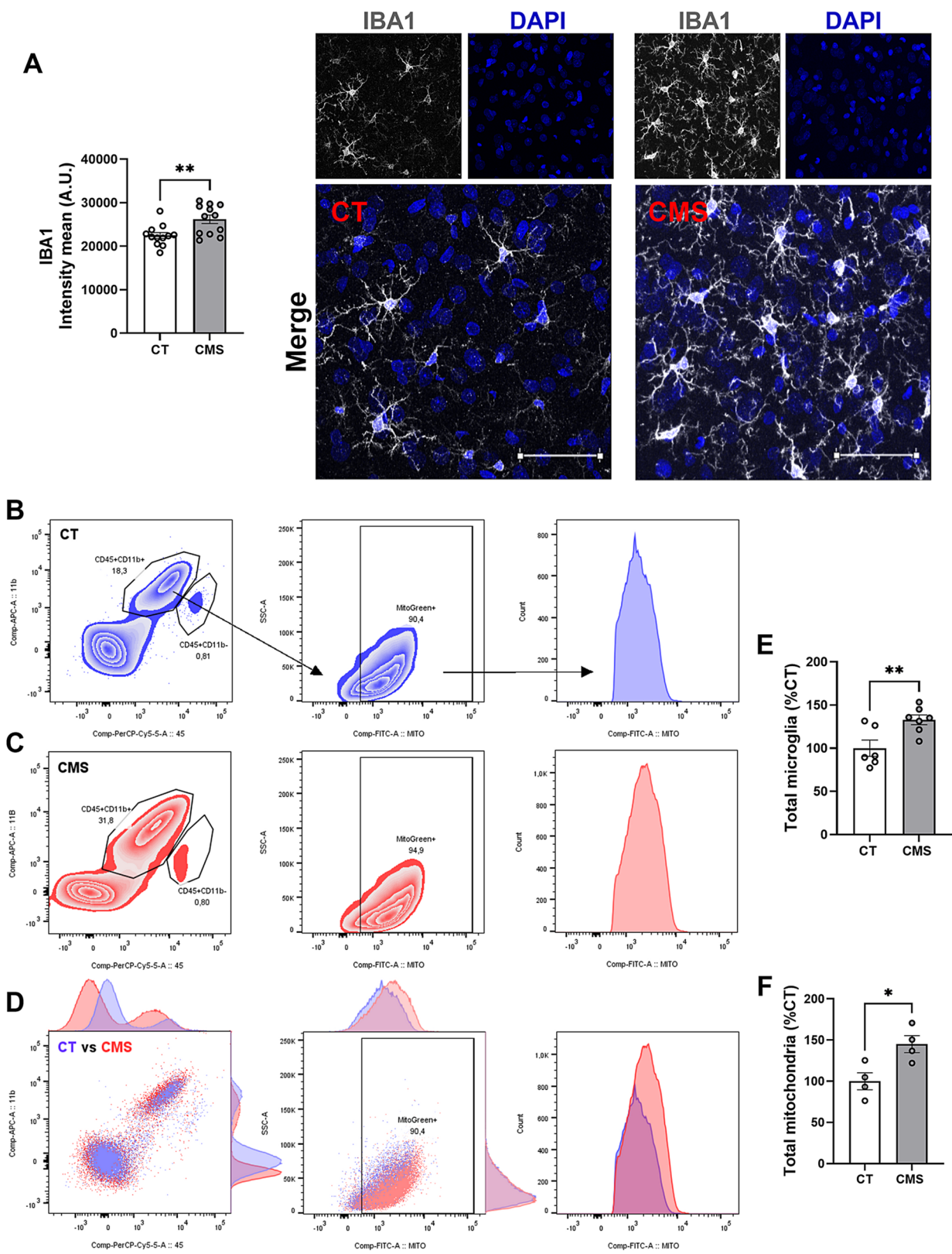


**Fig. 5** (See legend on next page.)

(See figure on previous page.)

**Fig. 5** CMS increased microglial population and their mitochondria in frontal cortex of rats. Microglia were assessed by IBA1 immunostaining in both groups. Scale bars represent 50  $\mu$ m. **(A)**. Microglia were then freshly isolated and incubated with CD45 and CD11b antibodies (x and y axis in the first column, respectively; CT group in purple and CMS group in red), and MitoTracker Green FM™ (x axis in the second and third columns) and analyzed by flow cytometry **(B–D)**. Overlapped CT and CMS microglial populations are displayed in **(D)**. CMS promoted microglial recruitment to the frontal cortex **(E)** and enhanced mitochondrial mass within them **(F)**. Two-tailed Student *t*-test was used for statistical analyses. Data is expressed as mean  $\pm$  SEM of 12–14 CT and CMS rats for immunofluorescence analysis, and 6 CT and CMS pools (containing frontal cortices of two rats per pool). Each plot had a starting cell number of 300,000 cells and live cells were never lower than 92%. (\*\**p* < 0.01)

the reason these potential protein changes are not yet observed at the nuclear level. The unaltered levels of *Rnr1*, *Nd1*, and *Nd5* would support this notion. What is more, the increase in *Pgc1 $\alpha$*  and *Nrf1* mRNA may reflect a compensatory response to the lower functional activity of PGC1 $\alpha$  protein in the nucleus. Moreover, the upregulation of PGC1 $\alpha$  prompts the generation of antioxidant enzymes to mitigate ROS concentrations and oxidative damage [66, 67]. Hence, PGC1 $\alpha$  modulation could have aided both control ROS and assist mitochondrial biogenesis.

Chronic inflammation drives microglia activation and recruitment under psychological stress, which is associated with changes in their morphology [68], and pro-inflammatory cytokines secretion [69]. Indeed, CMS triggered the increment of microglia levels in the FC, measured both by IBA1 and CD45-CD11b markers. Microglial activation has shown to be responsible for the CMS-induced anxiety- and depressive-like behavior [70], and thus, the role of microglial mitochondria was compelling to dive into.

CMS not only facilitates microglial recruitment but also promotes an increase in mitochondrial numbers within these cells, supporting the potential for targeted modulation of microglial mitochondria to control neuroinflammation. For instance, it has been reported that microglial PGC1 $\alpha$  ameliorates neuroinflammation by inhibiting the hyperactivation of the NLRP3 inflammasome in vitro [71]. The elevated mRNA levels of PGC1 $\alpha$  might be consequence of its role in neuroinflammation as well. Stress increases energy demand and, accordingly, the need of more mitochondria to respond and adapt to the stressful situation also escalates [46]. The prospect of chronic stress distinctly modulating mitochondria from each cell type in the CNS might suggest that glial and neuronal mitochondria could play a specific role in the stress response.

Prospective approaches should dig into the state of microglial mitophagy markers. In fact, it was observed that, depending on the inflammatory status, mitophagy-related effectors in periphery mononuclear blood cells (PBMC) from patients with MDD were altered and associated with the severity of the depressive symptomatology [72]. One study found that NIX-mediated mitophagy was impaired by inflammation signaling [73],

so mitophagy and neuroinflammation could be acting as mutual nemesis under stress conditions.

This work has some limitations: this study was only performed in male rats; electron microscopy experiments are needed to investigate the rise of CMS-derived mitochondrial mass considering size, morphology, and number; and certainly, the pharmacological intervention would allow the determination of the mitophagy flux, accompanied by some intracellular tracker to evaluate mitophagosome formation and fusion with lysosomes. Further characterization of microglial mitochondria is also paramount to understanding how mitochondrial dynamics and mitophagy work within this population and its interplay with the stress response. This study has strengths as well. It considered mitochondrial makers both in cytosolic and in mitochondrial-enriched fractions in the same samples of rat FC, allowing to compare soluble and mitochondrial protein presence, which is impossible to discern in total homogenates. Furthermore, the isolation and quantification of microglia populations in adult rat brain is exceedingly difficult to achieve, especially when it comes to obtaining elevated levels of healthy microglia. The determination of their mitochondrial mass is another milestone, which will be important to comprehend the role of mitochondria in the stress-derived neuroinflammation.

## Conclusions

CMS exposure resulted in the increment of mitochondrial mass, oxidative damage, the subsequent mitochondrial depolarization, and the alteration of mitochondrial dynamics in FC. Stress also induced PINK1, PARKIN, BNIP3, NIX, and FUNDC1 mitophagy proteins while accumulating mitochondria suggests that mitophagy is impaired at certain level. The CMS-generated neuroinflammatory environment derived in the enhancement of microglial recruitment and the elevation of their mitochondrial mass. The compilation of this data is shown in Fig. 6. Together, these data highlight the relevance of mitochondria in the CNS response to stress and the potential modulation of their status to control oxidative stress and neuroinflammation, two chief aspects in the pathophysiology of MDD. Therefore, our study reinforces the idea that comprehending the role of mitochondria in depression is crucial, illuminating potential avenues for

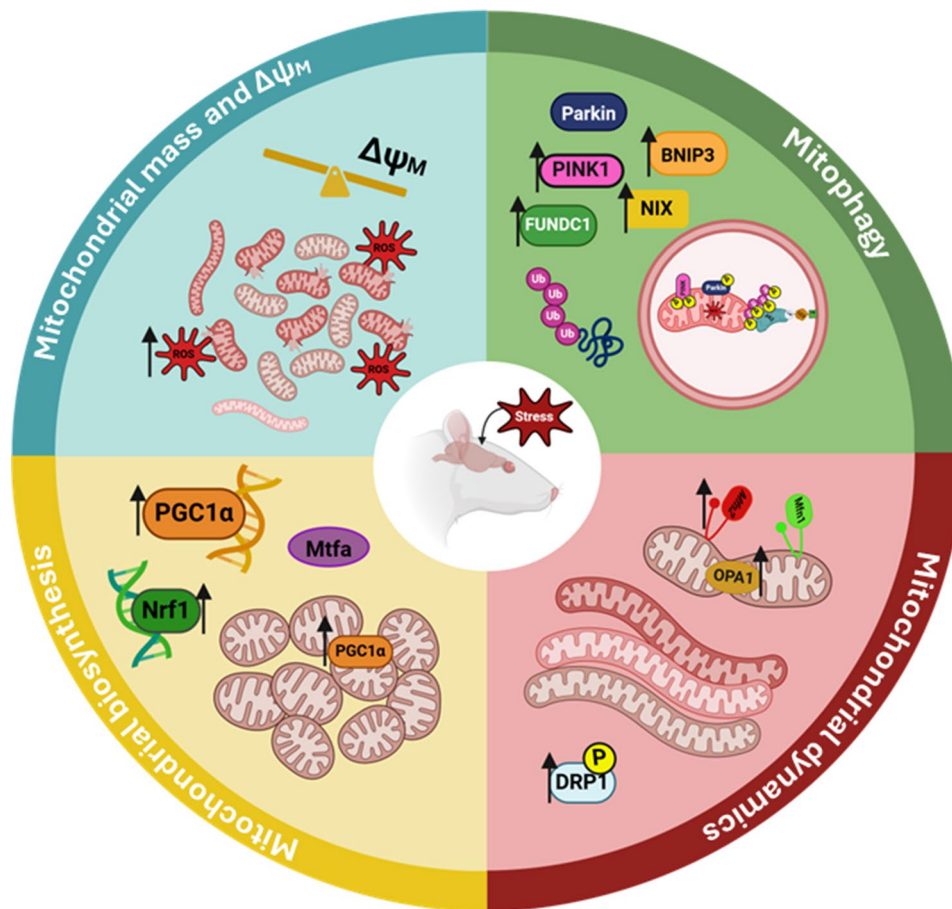


**Fig. 6** Schematic of Mitochondria-related alterations caused by the exposition to CMS in frontal cortex of adult rats

therapeutic interventions and underscoring the intricate link between cellular processes and neuropsychiatric diseases.

#### Abbreviations

8-OHdG	8-hydroxy-2-deoxyguanosine
ATP	Adenosine triphosphate
BNIP3	BCL2 interacting protein 3
BNIP3L/NIX	BCL2 interacting protein 3 like
CMS	Chronic mild stress
CNS	Central nervous system
CT	Control
DRP1	GTPase dynamin-related protein 1
FC	Frontal cortex
FUNDC1	FUN14 domain containing 1
IF	Immunofluorescence
IP	Immunoprecipitation
MDA	Malondialdehyde
MDD	Major depressive disorder
MFN1	Mitofusin 1
MFN2	Mitofusin 2
MTFA	Mitochondrial transcription factor A
Nd1	NADH dehydrogenase subunit 1
Nd5	NADH dehydrogenase subunit 5
NRF1	Nuclear respiratory factor 1
OMM	Outer mitochondrial membrane
OPA1	Optic atrophy protein 1
PBS	Phosphate-buffered saline
PGC1α	Peroxisome proliferator-activated receptor γ coactivator α

PINK1	Tensin homologue-induced putative kinase 1
Rnr1	Ribonucleotide reductase large subunit 1
RT-qPCR	Quantitative reverse transcription polymerase chain reaction
SQSTM1/p62	Sequestosome
TOMM20	Translocase of the outer mitochondrial membrane complex subunit 20
WB	Western blot

#### Supplementary Information

The online version contains supplementary material available at <https://doi.org/10.1186/s12967-025-06604-1>.

Supplementary Material 1

#### Acknowledgements

We would like to thank the Animal Facility as well as the Center for Microscopy and Flow Cytometry of the Complutense University of Madrid. We are also thankful to Ms. Beatriz Moreno for helping with the mitochondrial extraction protocols.

#### Author contributions

CUM: Investigation, Methodology, Writing– original draft, Writing– review & editing. AGB: Methodology, Writing– original draft. KSM: Investigation, Writing– original draft. JLMM and BGB: Methodology, Writing– review & editing. JCL: Funding acquisition, Writing– review & editing. JRC: Conceptualization, Funding acquisition, Supervision, Writing– review & editing.

## Funding

This work was supported by the Spain's Ministry of Science, Innovation and Universities, the *Agencia Estatal de Investigación* (MICIU/AEI/<https://doi.org/10.13039/501100011033>) and the European Regional Development Fund (FEDER), European Union (EU) [PID2020-113103RB-I00 and PID2023-146894NB-I00] and CIBERSAM-ISCIII [CB/07/09/0026]. CUM was a FPU fellow from the Spain's Ministry of Universities.

## Data availability

The datasets used and/or analysed during the current study are available from the corresponding author on reasonable request.

## Declarations

### Ethics approval and consent to participate

The animal studies were reviewed and approved by the Animal Welfare Committee of the Complutense University and approved by the Madrid Regional Government guidelines (PROEX098/19) according to European legislation (2010/63/EU).

### Consent for publication

Not applicable.

### Competing interests

The authors declare that they have no competing interests.

Received: 4 February 2025 / Accepted: 12 May 2025

Published online: 23 May 2025

## References

1. Chance B, Williams GR, Holmes WF, Higgins J. Respiratory enzymes in oxidative phosphorylation. V. A mechanism for oxidative phosphorylation. *J Biol Chem.* 1955;217:439–51.
2. Gallo LI, Lagadari M, Piwien-Pilipuk G, Galigniana MD. The 90-kDa heat-shock protein (Hsp90)-binding Immunophilin FKBP51 is a mitochondrial protein that translocates to the nucleus to protect cells against oxidative stress. *J Biol Chem.* 2011;286:30152–60.
3. Linnane AW, Marzuki S, Ozawa T, Tanaka M. Mitochondrial DNA mutations as an important contributor to ageing and degenerative diseases. *Lancet.* 1989;1:642–5.
4. Mukhopadhyay A, Ni L, Yang CS, Weiner H. Bacterial signal peptide recognizes HeLa cell mitochondrial import receptors and functions as a mitochondrial leader sequence. *Cell Mol Life Sci.* 2005;62:1890–9.
5. Reed JC, Jurgensmeier JM, Matsuyama S. Bcl-2 family proteins and mitochondria. *Biochim Biophys Acta.* 1998;1366:127–37.
6. Wong YC, Kim S, Peng W, Krainc D. Regulation and function of Mitochondria-Lysosome membrane contact sites in cellular homeostasis. *Trends Cell Biol.* 2019;29:500–13.
7. Rohas LM, St-Pierre J, Uldry M, Jager S, Handschin C, Spiegelman BM. A fundamental system of cellular energy homeostasis regulated by PGC-1 $\alpha$ . *Proc Natl Acad Sci U S A.* 2007;104:7933–8.
8. Nakahira K, Haspel JA, Rathinam VA, Lee SJ, Dolinay T, Lam HC, Englert JA, Rabinovitch M, Cernadas M, Kim HP, et al. Autophagy proteins regulate innate immune responses by inhibiting the release of mitochondrial DNA mediated by the NALP3 inflammasome. *Nat Immunol.* 2011;12:222–30.
9. Marques E, Kramer R, Ryan DG. Multifaceted mitochondria in innate immunity. *NPJ Metab Health Dis.* 2024;2:6.
10. Gkikas I, Palikaras K, Tavernarakis N. The role of mitophagy in innate immunity. *Front Immunol.* 2018;9:1283.
11. Devine MJ, Kittler JT. Mitochondria at the neuronal presynapse in health and disease. *Nat Rev Neurosci.* 2018;19:63–80.
12. Szabadkai G, Simoni AM, Chami M, Wieckowski MR, Youle RJ, Rizzuto R. Drp-1-dependent division of the mitochondrial network blocks intraorganelle Ca<sup>2+</sup> waves and protects against Ca<sup>2+</sup>-mediated apoptosis. *Mol Cell.* 2004;16:59–68.
13. Sun T, Qiao H, Pan PY, Chen Y, Sheng ZH. Motile axonal mitochondria contribute to the variability of presynaptic strength. *Cell Rep.* 2013;4:413–9.
14. Savitz JB, Price JL, Drevets WC. Neuropathological and neuromorphometric abnormalities in bipolar disorder: view from the medial prefrontal cortical network. *Neurosci Biobehav Rev.* 2014;42:132–47.
15. Matta SM, Hill-Yardin EL, Crack PJ. The influence of neuroinflammation in autism spectrum disorder. *Brain Behav Immun.* 2019;79:75–90.
16. Flatow J, Buckley P, Miller BJ. Meta-analysis of oxidative stress in schizophrenia. *Biol Psychiatry.* 2013;74:400–9.
17. Zorn JV, Schur RR, Boks MP, Kahn RS, Joels M, Vinkers CH. Cortisol stress reactivity across psychiatric disorders: A systematic review and meta-analysis. *Psychoneuroendocrinology.* 2017;77:25–36.
18. Kennis M, Gerritsen L, van Dalen M, Williams A, Cuijpers P, Bockting C. Prospective biomarkers of major depressive disorder: a systematic review and meta-analysis. *Mol Psychiatry.* 2020;25:321–38.
19. Picard M, Shirihai OS. Mitochondrial signal transduction. *Cell Metab.* 2022;34:1620–53.
20. Hunter RG, Seligsohn M, Rubin TG, Griffiths BB, Ozdemir Y, Pfaff DW, Datson NA, McEwen BS. Stress and corticosteroids regulate rat hippocampal mitochondrial DNA gene expression via the glucocorticoid receptor. *Proc Natl Acad Sci U S A.* 2016;113:9099–104.
21. Sequeira A, Rollins B, Magnan C, van Oven M, Baldi P, Myers RM, Barchas JD, Schatzberg AF, Watson SJ, Akil H, et al. Mitochondrial mutations in subjects with psychiatric disorders. *PLoS ONE.* 2015;10:e0127280.
22. Onishi H, Kawanishi C, Iwasawa T, Osaka H, Hanihara T, Inoue K, Yamada Y, Kosaka K. Depressive disorder due to mitochondrial transfer RNA<sup>Leu</sup>(UUR) mutation. *Biol Psychiatry.* 1997;41:1137–9.
23. Morava E, Gardeitchik T, Kozicz T, de Boer L, Koene S, de Vries MC, McFarland R, Roobol T, Rodenburg RJ, Verhaak CM. Depressive behaviour in children diagnosed with a mitochondrial disorder. *Mitochondrion.* 2010;10:528–33.
24. Andrieux P, Chevillard C, Cunha-Neto E, Nunes JPS. Mitochondria as a cellular hub in infection and inflammation. *Int J Mol Sci.* 2021;22.
25. Kubli DA, Gustafsson AB. Mitochondria and mitophagy: the Yin and Yang of cell death control. *Circ Res.* 2012;111:1208–21.
26. Kraus F, Roy K, Pucadyil TJ, Ryan MT. Function and regulation of the divisome for mitochondrial fission. *Nature.* 2021;590:57–66.
27. Gebara E, Zanoletti O, Ghosal S, Grosse J, Schneider BL, Knott G, Astori S, Sandi C. Mitofusin-2 in the nucleus accumbens regulates anxiety and Depression-like behaviors through mitochondrial and neuronal actions. *Biol Psychiatry.* 2021;89:1033–44.
28. Hasson SA, Kane LA, Yamano K, Huang CH, Sliter DA, Buehler E, Wang C, Heman-Ackah SM, Hessa T, Guha R, et al. High-content genome-wide RNAi screens identify regulators of parkin upstream of mitophagy. *Nature.* 2013;504:291–5.
29. Palikaras K, Lionaki E, Tavernarakis N. Mechanisms of mitophagy in cellular homeostasis, physiology and pathology. *Nat Cell Biol.* 2018;20:1013–22.
30. Onishi M, Yamano K, Sato M, Matsuda N, Okamoto K. Molecular mechanisms and physiological functions of mitophagy. *EMBO J.* 2021;40:e104705.
31. Tripathi A, Scaini G, Barichello T, Quevedo J, Pillai A. Mitophagy in depression: pathophysiology and treatment targets. *Mitochondrion.* 2021;61:1–10.
32. Ding WX, Ni HM, Li M, Liao Y, Chen X, Stolz DB, Dorn GW 2nd, Yin XM. Nix is critical to two distinct phases of mitophagy, reactive oxygen species-mediated autophagy induction and Parkin-ubiquitin-p62-mediated mitochondrial priming. *J Biol Chem.* 2010;285:27879–90.
33. Lee Y, Lee HY, Hanna RA, Gustafsson AB. Mitochondrial autophagy by Bnip3 involves Drp1-mediated mitochondrial fission and recruitment of parkin in cardiac myocytes. *Am J Physiol Heart Circ Physiol.* 2011;301:H1924–1931.
34. Chung JK, Lee SY, Park M, Joo EJ, Kim SA. Investigation of mitochondrial DNA copy number in patients with major depressive disorder. *Psychiatry Res.* 2019;282:112616.
35. Doblado L, Lueck C, Rey C, Samhan-Arias AK, Prieto I, Stacchiotti A, Monsalve M. Mitophagy in human diseases. *Int J Mol Sci.* 2021;22.
36. Shu X, Sun Y, Sun X, Zhou Y, Bian Y, Shu Z, Ding J, Lu M, Hu G. The effect of Fluoxetine on astrocyte autophagy flux and injured mitochondria clearance in a mouse model of depression. *Cell Death Dis.* 2019;10:577.
37. Jin X, Zhu L, Lu S, Li C, Bai M, Xu E, Shen J, Li Y. Baicalin ameliorates CUMS-induced depression-like behaviors through activating AMPK/PGC-1 $\alpha$  pathway and enhancing NIX-mediated mitophagy in mice. *Eur J Pharmacol.* 2023;938:175435.
38. Yang L, Ao Y, Li Y, Dai B, Li J, Duan W, Gao W, Zhao Z, Han Z, Guo R. Morinda officinalis oligosaccharides mitigate depression-like behaviors in hypertension rats by regulating Mfn2-mediated mitophagy. *J Neuroinflammation.* 2023;20:31.



39. Belleau EL, Treadway MT, Pizzagalli DA. The impact of stress and major depressive disorder on hippocampal and medial prefrontal cortex morphology. *Biol Psychiatry*. 2019;85:443–53.
40. Willner P. Chronic mild stress (CMS) revisited: consistency and behavioural-neurobiological concordance in the effects of CMS. *Neuropsychobiology*. 2005;52:90–110.
41. Bravo L, Mico JA, Rey-Brea R, Perez-Nievas B, Leza JC, Berrocoso E. Depressive-like States heighten the aversion to painful stimuli in a rat model of comorbid chronic pain and depression. *Anesthesiology*. 2012;117:613–25.
42. Martin-Hernandez D, Bris AG, MacDowell KS, Garcia-Bueno B, Madrigal JL, Leza JC, Caso JR. Modulation of the antioxidant nuclear factor (erythroid 2-derived)-like 2 pathway by antidepressants in rats. *Neuropharmacology*. 2016;103:79–91.
43. McCurdy RD, McGrath JJ, Mackay-Sim A. Validation of the comparative quantification method of real-time PCR analysis and a cautionary Tale of housekeeping gene selection. *Gene Ther Mol Biol*. 2008;12:1215–24.
44. Madrigal JL, Olivenza R, Moro MA, Lizasoain I, Lorenzo P, Rodrigo J, Leza JC. Glutathione depletion, lipid peroxidation and mitochondrial dysfunction are induced by chronic stress in rat brain. *Neuropsychopharmacology*. 2001;24:420–9.
45. Guo C, Ding P, Xie C, Ye C, Ye M, Pan C, Cao X, Zhang S, Zheng S. Potential application of the oxidative nucleic acid damage biomarkers in detection of diseases. *Oncotarget*. 2017;8:75767–77.
46. Picard M, McEwen BS, Epel ES, Sandi C. An energetic view of stress: focus on mitochondria. *Front Neuroendocrinol*. 2018;49:72–85.
47. Sivandzade F, Bhalerao A, Cucullo L. Analysis of the mitochondrial membrane potential using the cationic JC-1 dye as a sensitive fluorescent probe. *Bio Protoc*. 2019;9.
48. Mouli PK, Twig G, Shirihai OS. Frequency and selectivity of mitochondrial fusion are key to its quality maintenance function. *Biophys J*. 2009;96:3509–18.
49. Gilkerson R, De La Torre P, St Vallier S. Mitochondrial OMA1 and OPA1 as gatekeepers of organellar structure/function and cellular stress response. *Front Cell Dev Biol*. 2021;9:626117.
50. Leboucher GP, Tsai YC, Yang M, Shaw KC, Zhou M, Veenstra TD, Glickman MH, Weissman AM. Stress-induced phosphorylation and proteasomal degradation of Mitofusin 2 facilitates mitochondrial fragmentation and apoptosis. *Mol Cell*. 2012;47:547–57.
51. Chen W, Zhao H, Li Y. Mitochondrial dynamics in health and disease: mechanisms and potential targets. *Signal Transduct Target Ther*. 2023;8:333.
52. Adebayo M, Singh S, Singh AP, Dasgupta S. Mitochondrial fusion and fission: the fine-tune balance for cellular homeostasis. *FASEB J*. 2021;35:e21620.
53. Gilkerson R, Kaur H, Carrillo O, Ramos I. OMA1-Mediated mitochondrial dynamics balance organellar homeostasis upstream of cellular stress responses. *Int J Mol Sci*. 2024;25.
54. Ishihara N, Eura Y, Mihara K. Mitofusin 1 and 2 play distinct roles in mitochondrial fusion reactions via GTPase activity. *J Cell Sci*. 2004;117:6535–46.
55. Filadi R, Greotti E, Turacchio G, Luini A, Pozzan T, Pizzo P. Mitofusin 2 ablation increases Endoplasmic reticulum-mitochondria coupling. *Proc Natl Acad Sci U S A*. 2015;112:E2174–2181.
56. Casellas-Diaz S, Larramona-Arcas R, Rique-Pujol G, Tena-Morraya P, Muller-Sanchez C, Segarra-Mondejar M, Gavalda-Navarro A, Villarroja F, Reina M, Martinez-Estrada OM, Soriano FX. Mfn2 localization in the ER is necessary for its bioenergetic function and neuritic development. *EMBO Rep*. 2021;22:e51954.
57. Twig G, Elorza A, Molina AJ, Mohamed H, Wikstrom JD, Walzer G, Stiles L, Haigh SE, Katz S, Las G, et al. Fission and selective fusion govern mitochondrial segregation and elimination by autophagy. *EMBO J*. 2008;27:433–46.
58. Kamienieva I, Duszynski J, Szczepanowska J. Multitasking guardian of mitochondrial quality: parkin function and parkinson's disease. *Transl Neurodegener*. 2021;10:5.
59. Bingol B, Sheng M. Mechanisms of mitophagy: PINK1, Parkin, USP30 and beyond. *Free Radic Biol Med*. 2016;100:210–22.
60. Liu X, Hussain R, Mehmood K, Tang Z, Zhang H, Li Y. Mitochondrial-Endoplasmic reticulum Communication-Mediated oxidative stress and autophagy. *Biomed Res Int*. 2022;2022:6459585.
61. Liu R, Xu C, Zhang W, Cao Y, Ye J, Li B, Jia S, Weng L, Liu Y, Liu L, Zheng M. FUNDC1-mediated mitophagy and HIF1 $\alpha$  activation drives pulmonary hypertension during hypoxia. *Cell Death Dis*. 2022;13:634.
62. He YL, Li J, Gong SH, Cheng X, Zhao M, Cao Y, Zhao T, Zhao YQ, Fan M, Wu HT, et al. BNIP3 phosphorylation by JNK1/2 promotes mitophagy via enhancing its stability under hypoxia. *Cell Death Dis*. 2022;13:966.
63. Cadenas E, Davies KJ. Mitochondrial free radical generation, oxidative stress, and aging. *Free Radic Biol Med*. 2000;29:222–30.
64. Wang S, Long H, Hou L, Feng B, Ma Z, Wu Y, Zeng Y, Cai J, Zhang DW, Zhao G. The mitophagy pathway and its implications in human diseases. *Signal Transduct Target Ther*. 2023;8:304.
65. Jornayvaz FR, Shulman GI. Regulation of mitochondrial biogenesis. *Essays Biochem*. 2010;47:69–84.
66. Abu Shelbayeh O, Arroum T, Morris S, Busch KB. PGC-1 $\alpha$  is a master regulator of mitochondrial lifecycle and ROS stress response. *Antioxid (Basel)*. 2023;12.
67. Rius-Perez S, Torres-Cuevas I, Millan I, Ortega AL, Perez S. PGC-1 $\alpha$ , inflammation, and oxidative stress: an integrative view in metabolism. *Oxid Med Cell Longev*. 2020;2020:1452696.
68. Walker FR, Nilsson M, Jones K. Acute and chronic stress-induced disturbances of microglial plasticity, phenotype and function. *Curr Drug Targets*. 2013;14:1262–76.
69. Calcia MA, Bonsall DR, Bloomfield PS, Selvaraj S, Barichello T, Howes OD. Stress and neuroinflammation: a systematic review of the effects of stress on microglia and the implications for mental illness. *Psychopharmacology*. 2016;233:1637–50.
70. Wang YL, Han QQ, Gong WQ, Pan DH, Wang LZ, Hu W, Yang M, Li B, Yu J, Liu Q. Microglial activation mediates chronic mild stress-induced depressive- and anxiety-like behavior in adult rats. *J Neuroinflammation*. 2018;15:21.
71. Han B, Jiang W, Cui P, Zheng K, Dang C, Wang J, Li H, Chen L, Zhang R, Wang QM, et al. Microglial PGC-1 $\alpha$  protects against ischemic brain injury by suppressing neuroinflammation. *Genome Med*. 2021;13:47.
72. Scaini G, Mason BL, Diaz AP, Jha MK, Soares JC, Trivedi MH, Quevedo J. Dysregulation of mitochondrial dynamics, mitophagy and apoptosis in major depressive disorder: does inflammation play a role? *Mol Psychiatry*. 2022;27:1095–102.
73. Lu JJ, Wu PF, He JG, Li YK, Long LH, Yao XP, Yang JH, Chen HS, Zhang XN, Hu ZL, et al. BNIP3L/NIX-mediated mitophagy alleviates passive stress-coping behaviors induced by tumor necrosis factor- $\alpha$ . *Mol Psychiatry*. 2023;28:5062–76.

## Publisher's note

Springer Nature remains neutral with regard to jurisdictional claims in published maps and institutional affiliations.